Check for updates

Regional differences in soil stable isotopes and vibrational features at depth in three California grasslands

L. M. Wahab · S. S. Chacon · S. L. Kim ·
A. A. Berhe

Abstract There are major gaps in our understanding of how Mediterranean ecosystems will respond to anticipated changes in precipitation. In particular, limited data exists on the response of deep soil carbon dynamics to changes in climate. In this study we wanted to examine carbon and nitrogen dynamics between topsoils and subsoils along a precipitation gradient of California grasslands. We focused on organic matter composition across three California grassland sites, from a dry and hot regime (~300 mm precipitation; MAT: 14.6 °C) to a wet, cool regime (~2160 mm precipitation/year; MAT: 11.7 °C). We determined changes in total elemental concentrations of soil carbon and nitrogen, stable isotope composition ($\delta^{13}C$, $\delta^{15}N$), and composition of soil organic matter (SOM) as measured through Diffuse Reflectance Infrared Fourier Transformed Spectroscopy (DRIFTS) to 1 m soil depth. We measured carbon persistence in soil organic matter (SOM) based on beta (β), a parameter based on the slope of carbon isotope composition across depth and proxy for turnover. Further, we examined the relationship between $\delta^{15}N$ and C:N values to infer SOM's degree of microbial processing. As expected, we measured the greatest carbon stock at the surface of our wettest site, but carbon stocks in subsoils converged at Angelo and Sedgwick, the wettest and driest sites, respectively. Soils at depth (> 30 cm) at the wettest site, Angelo, had the lowest C:N and highest $\delta^{15}N$ values with the greatest proportion of simple plant-derived organic matter according to DRIFTS. These results suggest differing stabilization mechanisms of organic matter at depth across our study sites. We infer that the greatest stability was conferred by associations with reactive minerals at depth in our wettest site. In contrast, organic matter at our driest site, Sedgwick, was subject to the most microbial processing. Results from this study demonstrate that precipitation patterns have important implications for deep soil carbon storage, composition, and stability.

Keywords Biogeochemical cycles · Soil carbon · Precipitation · Grasslands

L. M. Wahab (✉) · S. S. Chacon · S. L. Kim · A. A. Berhe
Life and Environmental Sciences Department, University of CA – Merced, Merced, CA, USA
e-mail: lwahab@ucmerced.edu

Introduction

Grasslands account for 34% of the terrestrial carbon stock and are susceptible to global changes in precipitation and temperature patterns over the coming centuries (Bai and Cotrufo 2022). In California,

Springer

grasslands account for 15% of the land area, with native intact grasslands being one of the state's most threatened ecosystems (D'Antonio et al. 2002). Climate change is predicted to intensify the hydrologic cycle and increase temperatures globally (IPCC 2022). Shifts in the amount and timing of precipitation can potentially lead to loss of carbon stocks within grasslands since key biogeochemical processes, plant communities, and fungal communities are sensitive to environmental conditions (Chou et al. 2008; Deepika and Kothamasi 2015; Fay et al. 2002; Knapp 2002; Suttle et al. 2007). Plant community composition and diversity, especially in Mediterranean grasslands, are sensitive to shifts in precipitation patterns (Suttle et al. 2007; Suttle and Thomsen 2007). Further, increasing temperature is shown to decrease soil organic carbon (SOC) stock in grasslands through feedbacks with carbon degrading enzymes, such as ligninase and cellulase activity (Chen et al. 2020a, b). However, elevated pCO_2 is suggested to increase SOC stock in grasslands by triggering greater carbon allocation belowground (Terrer et al. 2021). This picture of changing SOC dynamics under climate change is further complicated once we integrate depth, leading to uncertainty regarding grassland carbon sequestration potential (Bai and Cotrufo 2022).

Subsoils (> 30 cm) store the majority of the of the global soil carbon pool (Jobbágy and Jackson 2000), but current measurements in the field of SOC and SOM stability are largely limited to topsoil (< 30 cm) (Yost and Hartemink 2020). The bias of current studies towards topsoil is typically due to greater access and abundance of organic matter and biomass in topsoils. However, more focus on subsoil SOM dynamics is warranted since subsoils are better suited to long-term carbon sequestration (Button et al. 2022) Physical, chemical, and biological factors important for understanding SOC stocks and stability vary between topsoils and subsoils, though to differing degrees depending on soil order (Button et al. 2022; Hicks Pries et al. 2023). These factors can include bulk density, pH, and Fe/Al oxide concentration, and are essential for understanding stabilization mechanisms and residence times of SOM across depths (Button et al. 2022). Under most conditions, SOM persistence tends to be greater in subsoils, as indicated by longer residence times based on radiocarbon measurements (Rumpel 2004). However, limited data exists on SOM

persistence in subsoils for soils across precipitation gradients. In this study, we define stability as the likelihood of organic matter to persist in soil rather than being decomposed, leached, eroded, and eventually respired as CO_2. Occlusion and mineral association act as physical and chemical mechanisms of stability, respectively, decreasing the likelihood of SOM being decomposed. A caveat is that roots and their exudates can impact the protective effects of occlusion and mineral association within the rhizosphere, and liberate organic carbon from protective associations (Jilling et al. 2018; Keiluweit et al. 2015; Schmidt et al. 2011). Field studies have the added benefit of providing realistic plant input and environmental fluctuation of subsoil carbon dynamics that are clearly needed for a better understanding of their sequestration potential under climate change as well as for their integration into models of SOM dynamics under changing environmental conditions.

Stable isotope composition, such as $\delta^{13}C$ and $\delta^{15}N$ can be informative in disentangling complex subsoil depth patterns. The natural abundance of carbon and nitrogen isotopes, specifically ^{13}C and ^{15}N, can be informative for several ecologically relevant processes on decadal and centennial timescales. For example, the vertical distribution of $\delta^{13}C$ values in soil profiles can be used to understand the balance between C3 and C4 grasses in an ecosystem, SOC processing, and microbial activity (Ehleringer et al. 2000; Staddon 2004; C. Wang et al. 2018). C3 plants in particular have a well-documented physiological response to increasing aridity that leads to high $\delta^{13}C$ values (Farquhar et al. 1989; Hartman and Danin 2010; Kohn 2010). This interaction between precipitation and the stable isotope content of plant matter means that the inputs for formed C will be affected by climate. The $\delta^{15}N$ values have also been shown to increase in arid environments, though the direct mechanism is less clear (Aranibar et al. 2004; Craine et al. 2015). Nitrogen inputs can occur through both atmospheric deposition and biological N_2 fixation. Inputs from biological fixation produce $\delta^{15}N$ values close to 0‰ (Högberg 1997; Robinson 2001), while per mille values from nitrogen deposition can have a wide range. Constraining the range of isotopic values for nitrogen deposition inputs is a current area of study due to increased nitrogen loading in ecosystems over time (Agnihotri et al. 2011; Chen, et al. 2020a, b). However, the vertical distribution of $\delta^{15}N$ values

is a useful proxy for SOM processing, and the balance between abiotic and biotic drivers of the nitrogen cycle (Conen et al. 2013; Hobbie and Ouimette, 2009a). The increase in $\delta^{13}C$ with depth in bulk soil are often attributed to a shift in microbial contributions from plant components, or changing inputs of fungal and microbial biomass with depth (Kohl et al. 2015). However, it is important to note that microbial fractionation during decomposition is what leads to ^{13}C enrichment of microbial biomass in comparison to plant tissues (Dijkstra et al. 2008). Disentangling the many interacting processes related to carbon and nitrogen cycling can be difficult because it can often mean detecting small changes in a large pool. However, integrative approaches using stable isotopes can be uniquely useful in quantifying and comparing ecosystem processes.

Relationships between C:N and $\delta^{15}N$ are linked to the processing and persistence of SOC and can be a useful proxy for disentangling depth patterns (Brunn et al. 2014; Conen et al. 2008, 2013). The transition from particulate organic matter (POM) to mineral-associated organic matter (MAOM) results in an inverse relationship. For example, low $\delta^{15}N$ value and high C:N can indicate POM, whereas higher $\delta^{15}N$ values and low C:N indicate MAOM, or greater stability (Conen et al. 2008). There is greater complexity underlying this continuum between POM and MAOM, and MAOM does not always correlate

with greater stability and persistence (Sokol et al. 2022). However, the inverse relationship between the $\delta^{15}N$ and C:N indicates nitrogen loss in ecosystems; "leaky" systems are indicated by higher C:N and $\delta^{15}N$ values as ^{14}N is lost during volatilization or denitrification (Conen et al. 2013). Isotope values and elemental concentrations can also discern nutrient turnover pools with indicators of SOM stability, such as β, the slope of $\delta^{13}C$, and log-transformed carbon concentration has good agreement with SOC turnover calculated from steady-state equations (Garten 2006). Previous studies indicate similar turnover results estimated using β and existing methods, such as radiocarbon age, and have related it to climatic factors, such as soil water conditions (Acton et al. 2013; Garten 2006) in global datasets (Wang et al. 2018) and chronosequences (Brunn et al. 2016). Overall, the natural abundance of stable isotopes provides valuable ecological information and enhance our ability to understand soil processes at a variety of depths and ecosystems, especially when paired with elemental carbon and nitrogen data and spectroscopic data.

In our study, we conducted soil measurements to 1 m depth across three California grasslands that exist along a climatic gradient to compare topsoil and subsoil SOM dynamics in three different climatic regimes (see the edaphic characteristics of each site in Table 1). A recent study at these sites showed that the climate gradient strongly influenced growing

Table 1 Description of study sites

	Angelo	Hopland	Sedgwick
MAP (mm/year)	126	58	24
MAT (C°)	11.7 ± 1.6	14.1 ± 1.6	14.6 ± 0.07
Temp Max/Min (C°)	20.4/4.6	22.0/9.0	19.7/9.0
Location coordinates	39° 44′ 20.58'' N	39° 0′ 1.6128'' N	34° 42′ 43.8876'' N
	− 123° 37′ 51.4956'' W	− 123° 5′ 30.6276'' W	− 120° 2′ 21.3936'' W
Elevation (m)	475	180	260
Soil Order	Alfisol	Mollisol	Mollisol
Soil Taxonomy	Ultic Haploxeralfs	Typic Argixerolls	Pachic Haploxerolls
pH	5.02	5.55	6.99
Sand/silt/clay (%)	28/42/27	45/36/19	38/28/34
NDVI	0.87	0.48	0.43

Temperature and precipitation data was sourced from California Irrigation Management Information systems (CIMIS) for Hopland and Sedgwick and Dendra (a cyber-infrastructure project for real time data storage) for Angelo. Mean annual precipitation and mean annual temperature data from 2012 to 2022 are reported. Temperature max/min refer to the mean maximum and minimum temperatures at each site. pH and textural information sourced from Foley et al. (2023) and are only measured for soils from 0 to 10 cm. NDVI was collected from MODIS data from 2020 and represents an annual average as proxy of plant inputs at each site

soil microbial communities and turnover rates based on soil $\Delta^{14}C$ (Foley et al. 2023); our study complements this dataset by examining stable isotopes and functional group chemistry to depth (1 m) at the same locations. We investigated the natural abundance of ^{13}C and ^{15}N, and isotopic proxies of stability and turnover in combination with Diffuse Reflectance Fourier Transform Spectroscopy (DRIFTS) to study the impact of both climatic factors and depth on soil carbon and nitrogen content and processes (Fig. 1).

Our study sought to answer three critical questions: (1) Are there variations in carbon concentration and stock between topsoil and subsoil across precipitation and temperature gradients? We hypothesized that soils in wetter climates would accrue more carbon in deeper soil layers due to high plant productivity and favorable mineralogy to retain carbon in deeper soils. (2) Are there differences in depth distributions of $\delta^{13}C$ and $\delta^{15}N$ stable isotopic signatures with varying climate? Additionally, do turnover and transformation
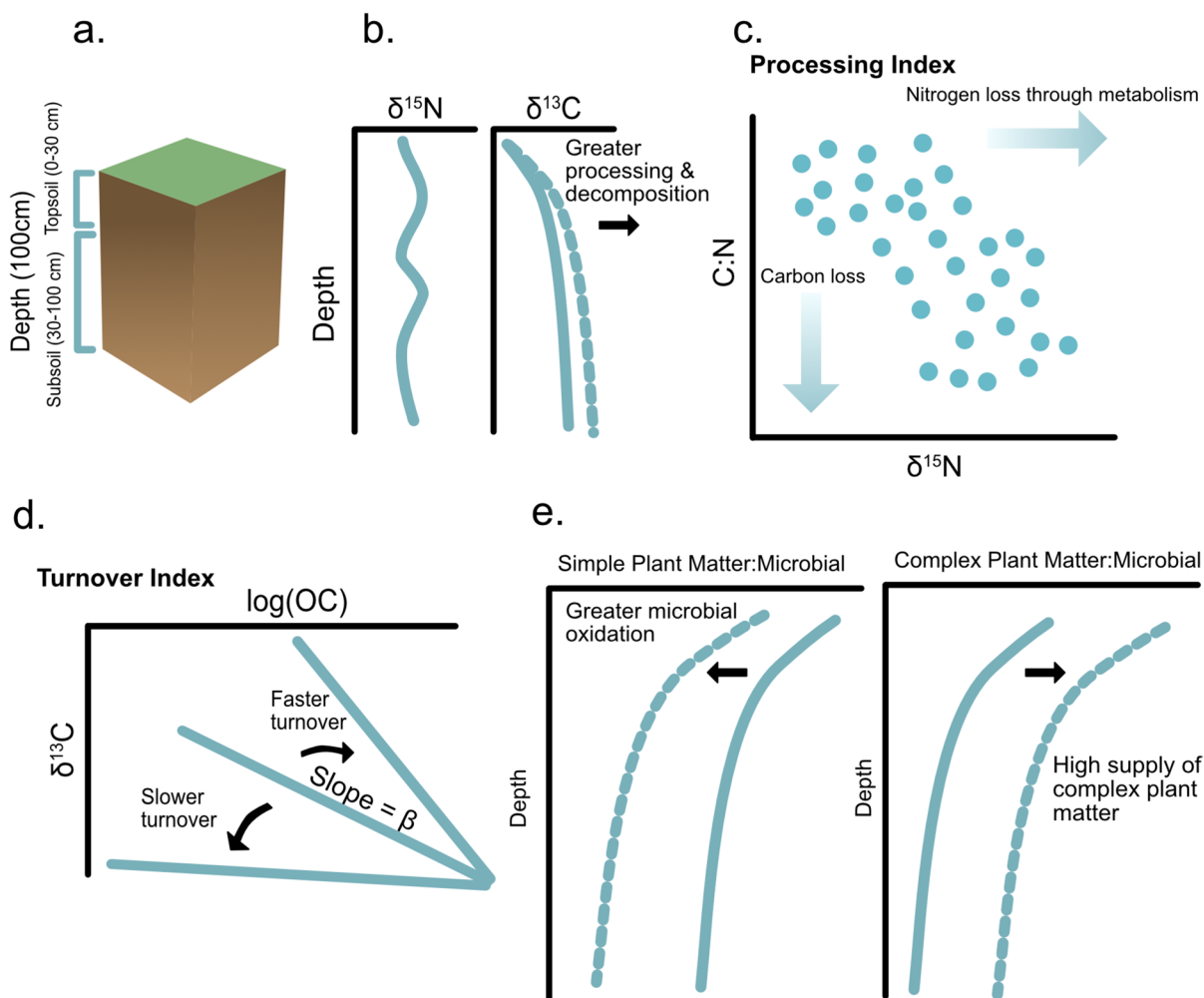

Fig. 1 Conceptual figure and overview of isotopic methodologies used in this study. Panel **a** indicates how we will define topsoil versus subsoil for our study, where topsoil refers to the top 30 cm. Panels **b–d** show the isotopic methodologies used in this study. Panel b shows depth profiles of stable isotope values, and our stable isotope measurements of interest ($\delta^{13}C$ and $\delta^{15}N$ on the x axes). Panel **c** shows an isotopic proxy we used for processing, termed our processing index, the relationship between $\delta^{15}N$ (x axis) and C:N (y axis). Panel d shows an isotopic proxy we used for turnover, beta, which is defined as the slope derived from relationship between the log transformed organic C (x axis) and $\delta^{13}C$ values (y axis). Panel e shows our interpretation of DRIFTS results, specifically our ratios of interest (simple plant matter: microbial and complex plant matter:microbial on the x axes) and how the represent biotic processes and input of simple and complex matter

Fig. 2 Map of three Mediterranean climate California annual grassland sites sampled for this study. (a) Geographic location of sites in California. (b-d) shows average monthly precipitation in mm from 2012 to 2022, with Mean Annual Precipitation over the same period indicated in parentheses by the label. Data was sourced from California Irrigation Management Information systems (CIMIS) for Hopland and Sedgwick and Dendra (a cyber-infrastructure project for real time data storage) for Angelo. Months are numbered, and plots start in July to center the wet season. (e) Average monthly temperatures for each site from 2012 to 2022
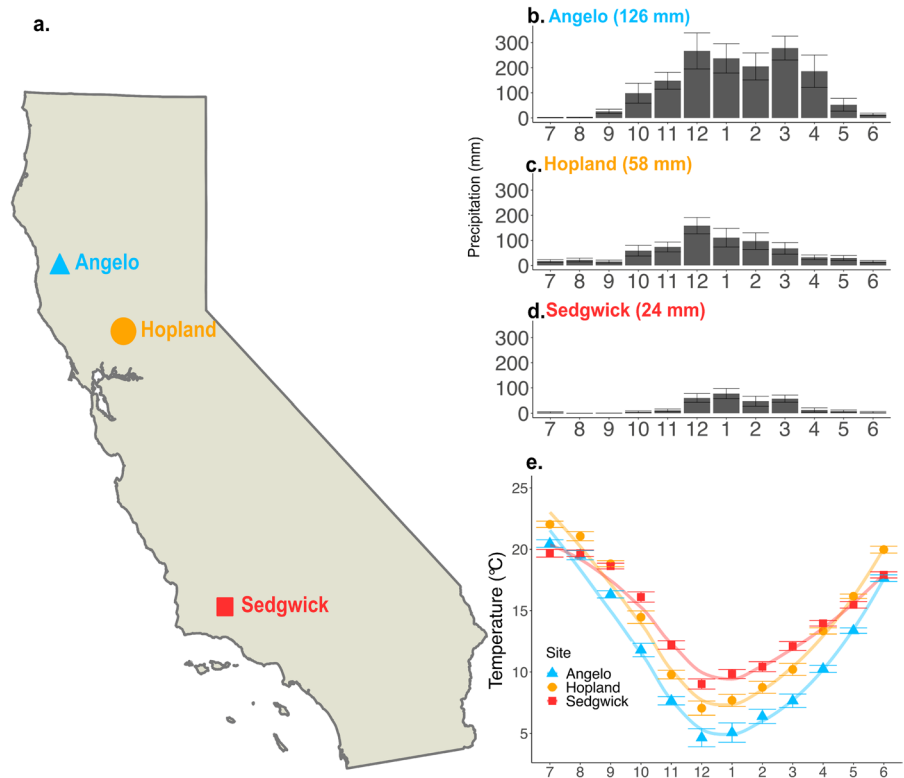
of organic matter vary between topsoil and subsoil across precipitation and temperature gradients? We hypothesized that topsoils would be enriched in ^{13}C and ^{15}N at our drier site. We also hypothesized that stable isotope signatures would be increased in subsoils at our wetter site, and would reflect a greater microbial signature. (3) Does the functional group chemistry of SOM vary across precipitation and temperature gradients and along depth profiles? Finally, regarding functional group chemistry, we hypothesized that there would be greater simple plant matter remaining in the profile at the driest site. We also hypothesized that there would be a greater proportion of microbially processed organic matter at the wettest site. Testing these hypotheses will provide crucial mechanistic knowledge of the role of soil moisture on soil formation and stabilization processes across sites and depths.

Materials and methods

Study area

Soil samples were collected at three annual grasslands: Sedgwick National Reserve (Suttle et al. 2007), University of California Hopland Research and Extension Center and the Angelo Coast Range Reserve in California (Fig. 2). Each site is an established reserve site within the University of California system, and, as such, has detailed information on vegetation and climatic factors. All three sites have not been exposed to agriculture, and do not have a history of C4 plants being present but are dominated by exotic annual grasses, while forbs are of both native and exotic origin. The dominant vegetation at Angelo is *Aira* spp., *Bromus* spp, and *Briza* spp. (Foley et al. 2023). At Hopland, it is a mix of *Avena* spp., *Bromus* spp., *Erodium* spp., and *Festuca* spp. (Foley et al. 2023). At Sedgwick, the dominant vegetation is *Avena* spp. and *Bromus* spp. (Foley et al. 2023). To further assess differences in plant communities, we aggregated all citations associated with plant surveys at each of our study sites (Supplemental Table 1). We

then further aggregated information about whether each species was C3/C4, native/introduced, or is a N-fixing or non-N-fixing plant. This helped us determine potential plant community impacts on isotopic values. Plant communities in this region are typically dominated by C3 annual grasses.

All soils across these sites have a xeric soil moisture regime (xer-), which indicates Mediterranean climates with wet, cool winters and warm, dry summers. At Angelo, soils are mapped as part of the Holohan-Hollowtree-Casabonne Complex, formed largely in gray wacke and mudstone. These are Alfisols with argillic (clay-enriched) or kandic (highly weathered clay) subsoil horizons (Ultic Haploxeralfs). At Hopland, soils were largely formed from sandstone and shale and are part of the Yorkville soil series; these are Mollisols with argillic subsoil horizons (Typic Argixerolls). We also observed redoximorphic features at Hopland in greater soil depths especially (~90 cm), specifically grey/white inclusions. Soils in upland areas exhibit redox features in deeper soils usually due to the presence of a fluctuating water table at depth. Soils at Sedgwick have been mapped as the Salinas soil series: Mollisols with the presence of calcium carbonate in subsoil horizons (Pachic Haploxerolls). Parent material is sandstone and shale at Sedgwick. There has been substantial discussion regarding the contributions of petrogenic carbon to soils from shale parent materials (Grant et al. 2023), which has been observed at Sedgwick (Bingham et al. 2021). Bingham et al. (2021) showed evidence of rock-derived nitrogen at depths greater than 1 m in Sedgwick soils, and saw increased $\delta^{15}N$ values (~6‰) associated with these inputs.

Experimental design and sampling

Soils were collected to 1 m across the three study sites, Angelo, Hopland, and Sedgwick. Samples at Hopland and Sedgwick were collected by hand auger to 1 m with 6–7 replicates per site, each site encompassing approximately 3 ha. We attempted to capture spatial heterogeneity but avoid confounding factors at each site by evenly sampling across similar slope positions (only Hopland had significant relief). At Angelo, samples were collected by Geoprobe due to being part of a different sampling campaign and were collected to depth of resistance (approximately 3 m) with 4 replicates. Depths greater than 1 m are

not reported for Angelo in this study. At all sites, soil samples were collected at consistent 10 cm intervals (0–10, 10–20, and so on).

After samples were collected, they were transported in coolers with ice packs and stored in a 4 °C cold room for approximately 4 months until they could be subsampled and analyzed. Long storage times occurred due to a lack of access to laboratory facilities due to the COVID-19 pandemic and subsequent shutdown procedures. When laboratories were opened and samples could be processed, a subsample was removed from each sample, and air dried for 7 days at room temperature. Soil samples were tested for carbonates by observing the presence and degree of effervescence with a few drops of 1 M Hydrochloric acid. Following air drying, the sample was then processed through a 2 mm sieve and a subsample was used for ball milling (using a Sample Prep 8000M Ball Mill) to a homogenous particle size. These homogenized samples were used for stable isotope and DRIFTS analysis.

We collected bulk density at Angelo and Hopland through Geoprobe cores, and calculated carbon stocks with these bulk density estimates. At Angelo, we subsampled each depth increment to estimate water content, and then calculated the dry mass of soil in a 10 cm increment. Bulk density was calculated as the mass of the dry > 2 mm fraction to correct for the impact of rock and root volume on soil carbon and nitrogen stocks (Throop et al. 2012). We did not observe a high contribution of coarse fraction at Hopland. At Sedgwick, due to difficulties with collecting bulk density cores at depth in an arid environment, we used a pedotransfer function to calculate bulk densities at this site. We used a pedotransfer function calibrated for Californian soils (Alexander 1980) that was recently evaluated to accurately estimate of bulk density (Abdelbaki 2018). The equation we used from Alexander (1980) to derive an estimate of bulk density at Sedgwick:

$$Bulk\ density\left(\frac{\text{g}}{\text{cm}^3}\right) = 1.66 - 0.308(OC)^{0.5} \qquad (1)$$

where OC represents concentration of organic carbon measured in bulk soils. This equation was recently evaluated to accurately estimate bulk density (Abdelbaki 2018). We further compared the results of this bulk density pedotransfer function on the estimated

versus measured carbon stocks at Angelo and Hopland (Fig. S1).

Elemental and isotopic analyses

Elemental and isotopic composition of carbon and nitrogen (i.e., %C, %N, $\delta^{13}C$, $\delta^{15}N$ values) in in all samples were measured in the Stable Isotope Ecosystem Laboratory at the University of California, Merced (SIELO). Briefly, samples were weighed into tin capsules and combusted in a Costech 4010 Elemental Analyzer coupled with a Delta V Plus Continuous Flow Isotope Ratio Mass Spectrometer. Carbon and nitrogen isotope compositions were corrected for instrumental drift, mass linearity, and standardized to the international VPDB ($\delta^{13}C$) and AIR ($\delta^{15}N$) scales using the USGS 41A and USGS 40 standard reference materials. Mean $\delta^{13}C$ values for reference materials were USGS $40 = -26.4 \pm 0.1‰$ (n = 173) and USGS $41a = 36.5 \pm 0.2‰$ (n = 87) and corresponding mean $\delta^{15}N$ values were USGS $40 - 4.5 \pm 0.1‰$ (n = 173) and USGS 41a $47.5 \pm 0.1‰$ (n = 87). Elemental carbon and nitrogen content were determined via linear regression of CO_2 and N_2 sample gas peak areas against the known carbon and nitrogen contents of USGS 40, USGS 41a, and Costech acetanilide. All isotope compositions are expressed in standard delta notations.

Diffuse reflectance infrared Fourier transform spectroscopy (DRIFTS)

To characterize the chemical composition of soil C across our study systems, we used Diffuse Reflectance mid-Infrared Fourier Transform spectroscopy (DRIFTS) analyses on bulk soil samples. DRIFTS measures the vibrational frequencies of functional groups found in soil organic matter and mineral surfaces. In addition, DRIFTS is informative on the abundance of organic and inorganic substances by measuring the excitation of molecular bonds when exposed to infrared radiation (Parikh et al. 2014). We used a Bruker IFS 66v/S Spectrophotometer (Ettlingen, Germany) with a praying Mantis apparatus (Harrick Scientific, Ossining, NY) at the Nuclear Magnetic Resonance (NMR) lab at UC Merced. Potassium bromide (KBr) was used as a background reference, but samples were not diluted with KBr. Samples were first dried in a desiccator following homogenization to remove interference from water. Absorption was measured between 4000 and 400 cm^{-1} averaged over 300 scans with an aperture of 4mm. Functional groups for simple plant carbon (aliphatic C–H; λ: 2976–2898 cm^{-1}), complex plant carbon (aromatic C=C; λ: 1550–1500 cm^{-1}), microbially derived carbon (amide/quinone/ketone, CO; aromatic, CC, carboxylate COO; λ: 1660–1580 cm^{-1}) were assigned following Mainka et al. (2022), also shown in Table 2 (Mainka et al. 2021; Parikh et al. 2014; Vranova et al. 2013). Simple plant-derived organic compounds are thought to originate from waxes as well as organic acids from plant roots, while complex plant matter originates from largely lignin and aromatic root exudates (Parikh et al. 2014; Ryals et al. 2014; Vranova et al. 2013). Microbial derived carbon more specifically originate from microbial cell wall constituents (Kögel-Knabner and Amelung 2014; Mainka et al. 2021). Wavenumbers that overlap with signals from mineral compounds (i.e., 1400–400 cm^{-1}), were excluded from the analysis (Margenot et al. 2015; Parikh et al. 2014). We also calculated ratios of simple plant carbon to microbial carbon, as well as complex plant carbon to microbial carbon. These ratios are helpful indicators of proportional contribution and biological processes; and a low ratio of simple plant carbon to microbial carbon indicates microbial oxidation of plant derived carbon and a high ratio of complex plant carbon to microbial carbon indicates

Table 2 Functional group assignments for the bands of interest used to evaluate DRIFT spectra. Based on Mainka et al. (2022)

Functional Group	SOM type	Wavenumber center (range) cm^{-1}
Aliphatic C–H stretch	Simple Plant Matter	2925 (2976–2998)
		2850 (2870–2839)
Aromatic C=C stretch	Complex Plant Matter	1525 (1550–1500)
Amide, quinone, ketone C=O stretch, aromatic C=C, and/or carboxylate C–O stretch	Microbially associated OM	1620 (1660–1580)

a high supply of aromatic plant compounds to soil (Fig. 1e).

Satellite-based remote sensing imager and processing MODIS imagery to calculate Normalized Difference Vegetation Index

Normalized Difference Vegetation Index (NDVI) is used to quantify vegetation greenness, and is used as a proxy for plant productivity. The NDVI ratio is an indicator of vegetation greenness, and a greater NDVI value indicates more greenness or greater plant productivity. We downloaded the Terra/MODIS surface reflectance (MOD09Q1.5) 8-day L3 global 250-m product from NASA's Earth Science Data System (https://www.earthdata.nasa.gov/) for the year 2020 (the same year sites were sampled) at all three sites in this study. This reflectance product provides a measure of surface reflectance at the ground level, and data were projected in a MODIS specific sinusoidal projection. These eight-day composite images represent the maximum surface reflectance over that time period while minimizing atmospheric effects, like clouds and aerosols. We used band 1 (620–670 nm) and band 2 (841–876 mm) to calculate NDVI over the entire MODIS image using the following equation:

$$NDVI = \frac{band2 - band1}{band2 + band1} \tag{2}$$

Afterward, we plotted data over the year 2020 (Fig. S2) and computed the average value over the entire year (Table 1).

## Statistical methods, calculation of turnover index (β values), and processing index

Differences in elemental, isotopic, and spectroscopic (DRIFTS data) parameters between sites within each 10 cm depth intervals were evaluated through a combination of one-way ANOVA and Tukey's HSD. To gain an initial sense of differences across sites, we used an ANOVA approach. However, greater spatial replication is needed to truly test whether site conditions are drivers of soil carbon stock and chemistry due to the pseudo replicated nature of our sampling regime. Measurements across sites within depth intervals were considered to be independent and sampled randomly through our sampling regime. We also assumed normality and homogeneity of variance within a depth interval within a site due to the random spatial sampling within sites. We did not apply an ANOVA and Tukey HSD to depth profiles within a site due to lack of independence of measurements within a depth profile. Any description of changes in isotopic or elemental parameters within a depth profile only refers to qualitative trends. Statistical significance was evaluated using $\alpha = 0.05$. All statistical analyses were performed in R.

The response of δ^{13}C values to SOC on logarithmic scale is termed β and is associated with isotopic fractionation due to decomposition and physical mixing (Acton et al. 2013). Using δ^{13}C values represents a natural (unlabeled) and high throughput methodology for measuring carbon accumulation and turnover dynamics across varied ecosystems (Acton et al. 2013). β is comparable to established techniques for measuring turnover, like radiocarbon measurements. β values indicate the rate that SOC δ^{13}C values vary with depth (Acton et al. 2013; Garten 2006; Garten and Hanson 2006) and change based on environmental factors, such as soil texture and soil water conditions (Campbell et al. 2009).The β values were derived from the slopes of linear regressions between log transformed C concentration (log (C%)) and their respective δ^{13}C values (‰ VPDB). In this case, the β values can be interpreted as the change in δ^{13}C for every tenfold increase in SOC content, and is indicative of isotopic fractionation during decomposition and recycling of SOC (Acton et al. 2013; Brunn et al. 2014; Garten and Hanson 2006). In this study, we interpreted steeper slopes, or greater β values, as greater turnover through decomposition or physical mixing, as it is indicative of processed litter.

A complementary indicator to soil turnover (β) is relating C:N (calculated on a weight basis) and δ^{15}N values to evaluate organic matter processing. Previous studies show this relationship is related to residual organic material that has undergone a greater degree of microbial processing, and that is likely becoming increasingly mineral associated (Brunn et al. 2014; Conen et al. 2008, 2013). While some studies have found that systems with substantial short range order oxide concentrations tend to have low C:N and low δ^{15}N in the densest and most stable fractions (Sollins et al. 2006, 2009), most studies suggest low δ^{15}N and high C:N in bulk soil as less processed. Here, we interpret high δ^{15}N and low C:N values as indicative

Fig. 3 a–e Elemental and isotopic variations in soils collected with depth across a precipitation gradient of three CA annual grasslands (from wetter to drier, Angelo > Hopland > Sedgwick). Plots show averages with standard error calculated for each 10 cm depth interval (n = 7 for Hopland and Sedgwick, n = 4 for Angelo) and represent within site sampling. Stars indicate significant differences (p < 0.05) according to one-way ANOVA by depth interval
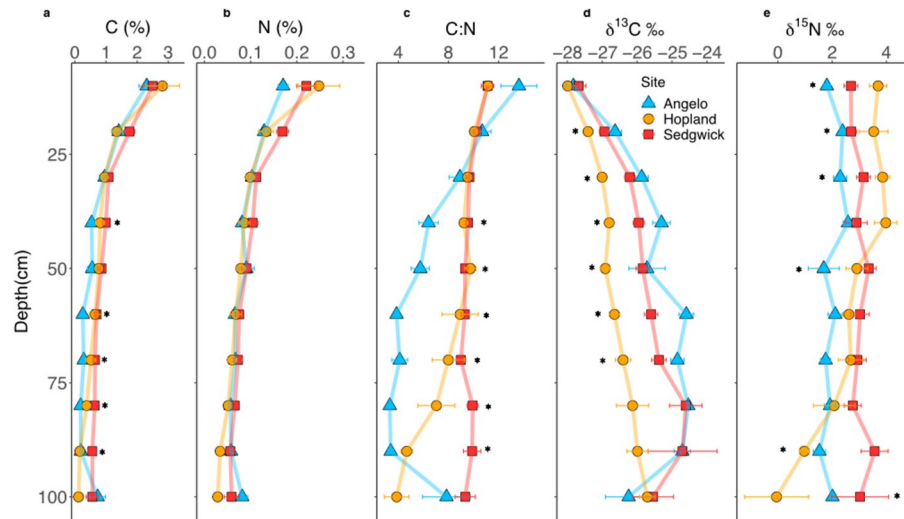
of more processed soil carbon, and low $\delta^{15}N$ and high C:N as less processed soil carbon.

We consider both the proxy β and the relationship between C:N and $\delta^{15}N$ values to be complementary indices for soil turnover, rates of decomposition, and physical/chemical protection of soil carbon. More specifically, we interpreted β (hereafter termed our turnover index) as processing due to decomposition and mixing, whereas the relationship between $\delta^{15}N$ and C:N (hereafter termed our processing index) is related to physical and/or chemical protection of soil carbon and decomposition through microbial metabolism.

Results

Elemental data across the precipitation gradient of ecosystems

When evaluating concentrations of carbon and nitrogen in soil at each of the sites, we observed important differences in C:N ratios across the three sites. We determined that total carbon = organic carbon in all our sites as testing with 1.0 M Hydrochloric acid resulted in no effervescence, indicating that the contribution of carbonates to total organic carbon was minimal even in soils mapped as the Salina soil series in Sedgwick. In topsoils (0–30 cm), we didn't detect significant differences in carbon and nitrogen concentrations between sites (Fig. 2a, b). However, carbon concentrations started to differ at 40 cm depth

(p < 0.05) (Fig. 2a). The largest difference in subsoils carbon and nitrogen concentrations, and hence C:N ratio was observed between our wet and dry sites, Angelo and Sedgwick, respectively, especially at 40 cm and, between 60 and 90 cm (p < 0.05). Nitrogen concentration was similar between all sites (Fig. 2b), and converged to similar nitrogen concentrations from 15 to 75 cm (~0.06%). We observed C:N ratios ranging from 10 to 12 at Hopland and Sedgwick for most of the depth profile. At Angelo, lower C:N ratios were detected for the majority of its profile (Fig. 2c), which was significantly different from the other sites (p < 0.0001) and persisted throughout the depth profile (50–90 cm). Carbon stocks were significantly higher at Angelo and Hopland in topsoils (0–30 cm) (Fig. 3). In subsoils, however, Sedgwick and Angelo had relatively similar carbon stocks. Hopland had the greatest subsoil carbon stocks. However, interpretation of carbon stock results from Sedgwick should be tempered due to the use of a pedotransfer function that used carbon concentrations to estimate bulk density at this site. For this reason, we discussed both concentrations and stocks of carbon at all sites. Overall, differences between sites were related to C:N ratios and carbon stocks, largely driven by low carbon concentrations and stocks at depth at Angelo (the wettest site).

Isotopic data across the precipitation gradient of ecosystems

All sites had similar $\delta^{13}C$ values at the surface but differences emerged at 20 cm and continued until 50 cm between Angelo and Hopland (Fig. 2d). Angelo had the greatest values between 30 and 70 cm ($-25 \pm 0.2‰$) and Hopland had the lowest values ($-27 \pm 0.1‰$) within this depth profile (Fig. 2d). At 60 cm, we observed differences in $\delta^{13}C$ values between all sites ($p < 0.0001$). However, nitrogen isotope patterns were more consistent within sites and there were no clear differences between topsoils and subsoils. Overall, Hopland had the greatest $\delta^{15}N$ values ($3.7 \pm 0.3‰$), Sedgwick ($2.7 \pm 0.2‰$) had intermediate values, and Angelo had the lowest values ($1.8 \pm 0.1‰$) (Fig. 2e). Hopland differed significantly in $\delta^{15}N$ value from both Angelo and Sedgwick at 10 cm, an effect that persisted to 30 cm ($p < 0.0001$). Although the $\delta^{15}N$ values at Hopland were initially greater than Sedgwick, at 50 cm this pattern switched and Sedgwick $\delta^{15}N$ values at depth were greater than Angelo for the deeper depths (Fig. 2e). However, there were no statistical differences among sites in $\delta^{15}N$ between 50 and 90 cm. Sites did differ significantly in $\delta^{15}N$ values at 100 cm ($p < 0.05$). Overall, we observed the greatest differences in isotope composition in the $\delta^{13}C$ values between sites, and between topsoils and subsoils, suggesting complex and interactive effects of climate with carbon cycling at depth.

Indices of turnover and proccessing and correlations with depth

Processing and turnover proxies were based on elemental and isotopic compositions at each site and across depth profiles. The turnover index, β, used elemental and isotopic data to discern the rate of change in $\delta^{13}C$ values with log-transformed C concentration. All localities in this study had different and negative β values (Fig. 5). Sedgwick, the warmest and driest site (MAT: 14.6 °C; MAP: ~300 mm precipitation/year), had the greatest β value of -1.8 ($R^2 = 0.89$, $p < 0.001$) followed by Angelo, the coolest and wettest site (MAT: 11.7 °C; MAP: ~2160 mm precipitation/year) with β value of -1.2 ($R^2 = 0.93$, $p < 0.001$). Hopland with intermediate temperature and precipitation (MAT: X; MAP: Y) had the lowest β value of -0.70
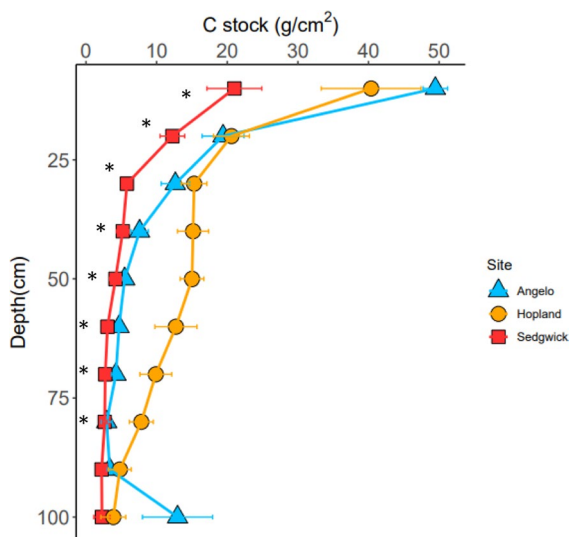

Fig. 4 Carbon stock data in soils collected with depth across a precipitation gradient of three CA annual grasslands (from wetter to drier, Angelo > Hopland > Sedgwick). Plots show averages with standard error calculated for each 10 cm depth interval (n = 3 for Hopland and n = 4 for Angelo). Stars indicate significant differences (p < 0.05) according to one-way ANOVA by depth interval. Carbon stocks at Angelo and Hopland were calculated based on geoprobe cores, whereas data at Sedgwick was calculated through a pedo-transfer function

and best fit ($R^2 = 0.94$, $p < 0.001$) (Fig. 5). Overall, the turnover index, β, was the greatest at our driest and warmest site and lowest at our intermediate site.

In contrast to the turnover index, the index used to discern SOM processing was based on $\delta^{15}N$ values versus C:N ratios, which highlighted unique relationships per field site (Fig. 6a–c). At Angelo, surface samples (from 0 to 30 cm) had high C:N (8–10) and $\delta^{15}N$ values (Fig. 6a) while samples at depth (> 30 cm) had much lower C:N values (~4 to 5) (Fig. 6a). At Hopland and Sedgwick, we did not observe a strong separation by depth category for C:N or $\delta^{15}N$ values (Figs. 6b, 3c). Specifically at Hopland, surface samples and samples at depth separated more weakly by C:N values (Fig. 6b), while at Sedgwick, all samples at all depths clustered around similar C:N values, and there was no consistent variation of depth with either C:N or $\delta^{15}N$ values (Fig. 6c). Strikingly, Angelo was the only site with strong depth separation for our processing indicator.

Fig. 5 a variations in soil β values for three CA annual grasslands across a precipitation gradient. R^2 is the coefficient of determination for each regression line. **b** is a conceptual diagram for interpretations of beta. Beta values represent the slope between the log of organic carbon and $\delta^{13}C$ values, thought to be indicative of turnover time of soil (Brunn et al. 2016) (n = 7 for Hopland and Sedgwick, n = 4 for Angelo). We interpreted beta as our turnover index. The regression lines are based on the averages for each set of depth replicates
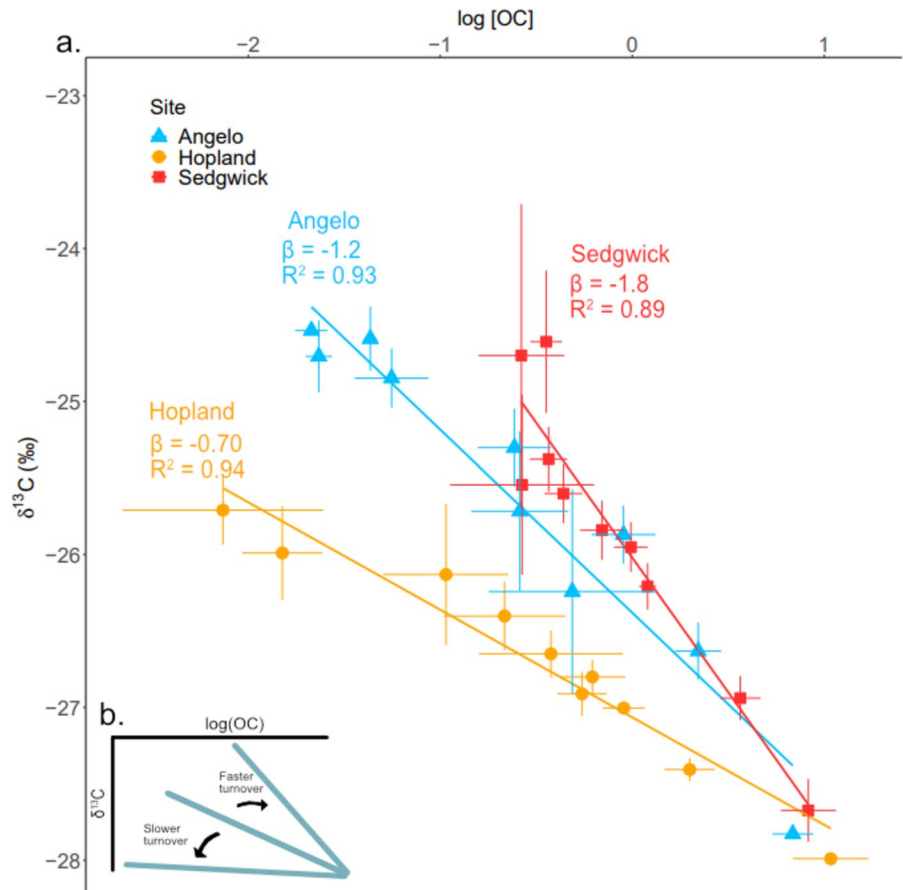
Predominant chemical moieties of organic carbon shifts across sites and depth

DRIFTS indicates functional group differences of organic matter across sites (Fig. 7). The proportion of functional groups categorized as simple plant-derived OM was generally higher in Angelo soils than at Sedgwick and Hopland, with higher proportions detected below 60 cm depths (Fig. 8a, $p < 0.05$). Significant differences in the complex plant-derived OM were not detected above 30 cm across all sites; significant shifts occurred for complex plant C below 50 cm (Fig. 8b, $p < 0.05$). Hopland soils had higher proportions of complex plant-derived OM at 70 and 90 cm depths than Angelo and Sedgwick soils ($p < 0.05$); meanwhile, Angelo soils started to decrease at 60 cm ($p < 0.05$). The proportion of microbially derived OM was significantly lower across all depths in Angelo soils when compared to the other sites (Fig. 8d, $p < 0.05$). No significant differences in microbially

derived OM were detected between Sedgwick and Hopland soils throughout the entire soil profile. The combination of lower proportion of microbially associated OM and higher proportion of simple plant-derived compounds at Angelo resulted in a greater simple plant matter to microbially associated OM ratio (Fig. 8d, $p < 0.05$). Sites all had a similar complex plant matter to microbial OM ratio, and there were almost no statistically significant differences except at 40 cm (Fig. 8e).

Differences in plant productivity across the gradient as indicated by NDVI

NDVI was greatest at the wettest site, Angelo, and similar between Hopland and Sedgwick (Table 1). We also observed seasonal variability in NDVI at Hopland and Sedgwick, with the greatest NDVI occurring in the spring months (Mar-Apr) and decreasing from the summer to winter (Jun-Dec)
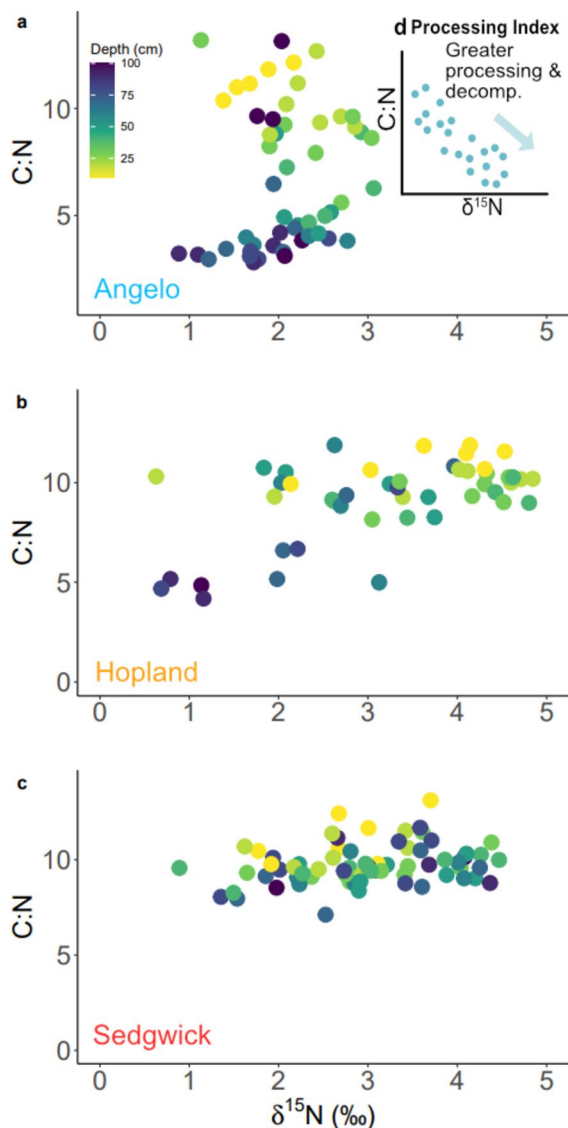
Fig. 6 a–d C:N versus $\delta^{15}N$ values for each site. All samples are plotted, and color scale indicates depth of sample (lighter = shallower, darker = deeper). We interpreted the distribution of C:N vs $\delta^{15}N$ as our stability index, and plotted these for **a** Angelo, **b** Hopland, and **c** Hopland. Part d is a conceptual diagram indicating an interpretation for the relationship between C:N and $\delta^{15}N$ values

(Fig. S2). Angelo had a consistently high (~0.9) NDVI throughout the year (Fig. S2).

Discussion

Elemental data from our sites, including carbon and nitrogen concentrations, C:N ratios, and carbon stocks indicated differences balance of carbon inputs and outputs at each site, providing clues for difference in mechanisms of SOM stabilization across our sites. The wettest site, Angelo, had the greatest surface carbon stocks but also the greatest proportion of simple plant-derived OM in subsoils. Our intermediate site, Hopland, had visual evidence of redox sites, and these were also indicated by greater heterogeneity in functional groups present and low $\delta^{13}C$ values. And finally, our driest site, Sedgwick, had the highest turnover and least differentiation between topsoils versus subsoils based on our processing indicator. Our results highlight the importance of considering regional differences in processing and turnover of subsoils for carbon sequestration efforts.

Elemental variations indicate different inputs to stable carbon pools

The greatest elemental variations were between C:N values and carbon stocks between sites. We observed the greatest carbon concentration (C%) across the depth profile at Sedgwick, the driest locality of our three sites (MAP: 24 mm/year; Fig. 2a) whereas the wettest site Angelo (MAP: 126 mm/year), had the lowest C:N values, especially at depth. We hypothesized the wettest sites would have the greatest carbon and nitrogen concentrations due to greater biomass input (Aranibar et al. 2004), which would also result in higher C:N; however our results did not conform to this simplistic schema. We observed greater plant inputs at Angelo through NDVI (Table 1) and greater surface stocks from our results, but subsoil carbon stocks were relatively similar between our wettest and driest site (Fig. 3). The slightly greater carbon concentration (C%) in subsoils at Sedgwick is consistent with conclusions of recent studies that dry conditions lead to lower decomposition rates (Berthrong et al. 2012; Campo and Merino 2016; Chai et al. 2022; Fröberg et al. 2008; Heckman et al. 2023; Zhang et al. 2015), but carbon accrual in dry conditions would be expected to be dampened by decreasing plant litter inputs. However, we observed relatively similar subsoil carbon stocks between Angelo and Sedgwick (Fig. 3). In a recent meta-analysis, decreased

Fig. 7 a–c DRIFTS spectra across sites and depths labelled with wavenumbers of interest. 2976–2998 cm^{-1} and 2870–2839 cm^{-1} represent aliphatic compounds and simple plant matter. 1550–1500 cm^{-1} represents aromatic compounds and complex plant matter. Finally, 1660–1580 cm^{-1} represents amide, quinone, ketone stretch, aromatic and/or carboxylate stretch, and microbially associated OM
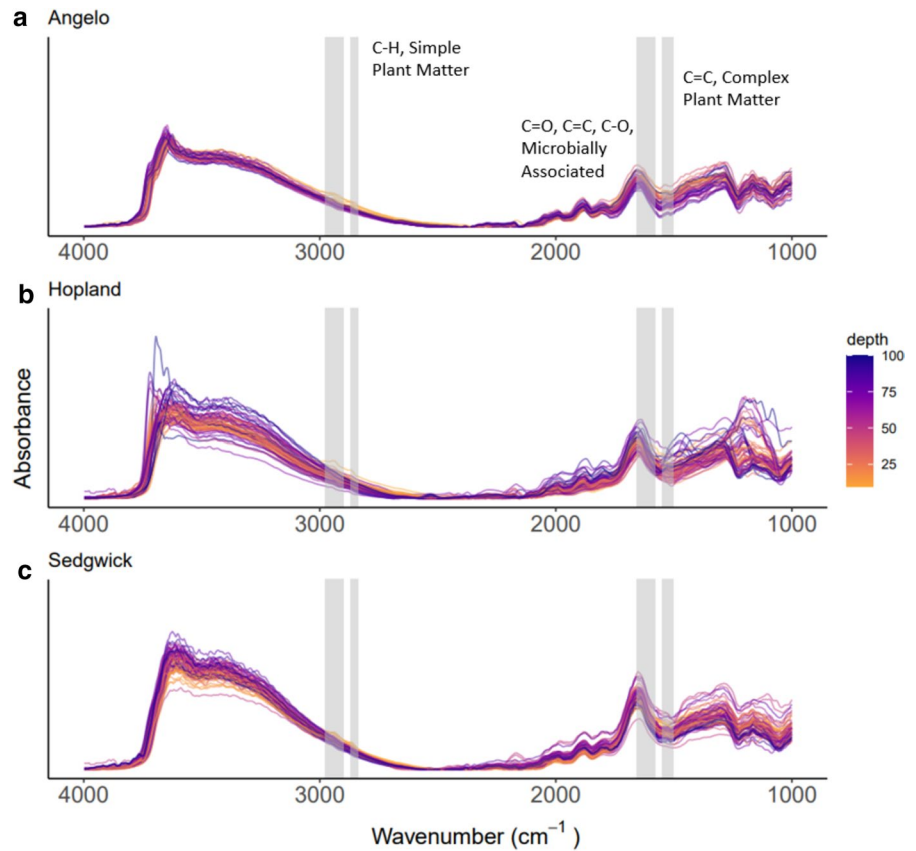
precipitation slowed carbon cycling processes across a wide gradient of ecosystems; semi-arid and temperate grasslands were particularly sensitive to increased precipitation (Song et al. 2019). Furthermore, there is evidence from manipulation studies that increased precipitation affects ecosystem carbon balance in grasslands due to increases in soil respiration (Chou et al. 2008; Harper et al. 2005). This interaction between precipitation and carbon balance is further complicated by carbon stock trends with depth at our sites. We observed the greatest carbon stocks in topsoils (0–30 cm) at the wet and intermediate site. However, we noted that the wet and dry sites approached similar carbon stock values deeper in the subsoils profile (below 30 cm); in contrast, our intermediate site actually had the greatest carbon stock in subsoils below 30 cm (Fig. 3). The effects of changing climatic dynamics are further complicated by including the effects of warming, which has been shown to decrease POM (Rocci et al. 2021) and enhance the formation of newly synthesized carbon in subsoils (Jia et al. 2019). Overall, we observed key differences

in C:N ratio and carbon stocks between topsoils and subsoils across ecosystems.

While carbon signals across sites clearly differed, it is crucial to consider carbon and nitrogen together due to the impact of nitrogen limitation in modulating plant and microbial activity. There is evidence of asymmetric responses to climatic regime changes that could affect soil carbon and nitrogen composition and/or cycling. For example, a precipitation manipulation study in a shortgrass steppe ecosystem found that long term drought significantly reduced CO_2 flux and caused accumulation of inorganic nitrogen (Evans and Burke 2013). This previous study suggests a decoupling of carbon and nitrogen cycling resulting in the observation that nitrogen mineralization and decomposition may have different sensitivities to moisture (Evans and Burke, 2013). In addition, field experiments in agricultural grassland ecosystems indicate decoupled carbon and nitrogen persistence as mineral associated carbon in necromass declines more rapidly than nitrogen (Buckeridge et al. 2022). This is likely occurring at Angelo, as indicated by
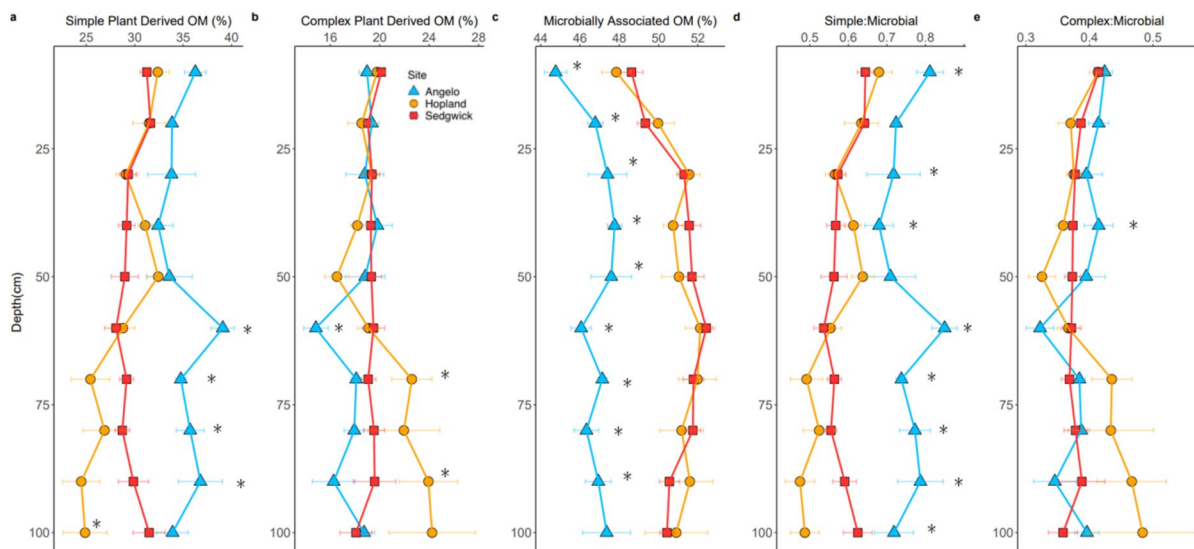
Fig. 8 a–e Proportions of integrated area for areas of interest in DRIFTS data. Panel **a** show the proportion of simple plant derived functional groups (2976–2998 cm^{-1} and 2870–2839 cm^{-1}), panel **b** shows the proportion of complex plant derived functional groups (1550–1500 cm^{-1}), and panel **c** shows the proportion of microbially associated OM (1660–1580 cm$^-$) for each site. Panels **d** and **e** show ratios of simple plant matter to microbial plant matter, and complex plant matter to microbial plant matter respectively. Plots show averages with standard error calculated for each 10 cm depth interval (n=7 for Hopland and Sedgwick, n=4 for Angelo), and represent within site sampling. Stars indicate significant differences (p<0.05) according to one-way ANOVA by 10 cm depth interval

low C:N values at depth (Fig. 2c) and differing functional group character as indicated by high proportions of simple plant-derived OM throughout the profile (Fig. 8d).

Historical, elemental, and functional group data in subsoils allowed us to make some inferences regarding stabilization mechanisms for carbon in these ecosystems. We hypothesized that we would see the greatest persistence of simple plant matter at the driest site, and greater evidence for microbial oxidation at the wettest site. However, the greatest ratio of simple to microbially associated OM was in Angelo subsoils (Fig. 8e) while the ratio of complex to microbial associated OM was similar across all sites. We expected greater microbial oxidation at our wettest site, but instead DRIFTS results provided the greatest evidence of this at our dry and intermediate site through DRIFTS. Overall, there was greater persistence of plant inputs throughout the profile at Angelo (Fig. 8a). Soils at Angelo are rich in Fe/Al short range order mineral surfaces (SRO) (Berhe et al. 2012) while soils at Sedgwick have no measurable Al minerals (Foley et al. 2023). Soils at Sedgwick also have the greatest surface clay content (Table 1) and a

greater base cation concentration (Foley et al. 2023). These base cations serve as a key stabilization mechanism due to cation bridging between OM and mineral surfaces (Aquino et al. 2011). Our results suggest greater persistence of microbial byproducts and plant inputs at Angelo, which could be contributing to mineral associated organic matter (MAOM) at depth. Stabilization at Sedgwick is likely driven by clay content and greater base cation concentrations that facilitate MAOM formation through cation bridging. We also saw greater evidence of microbial oxidation at depth in Sedgwick with DRIFTS, which is consistent with its high turnover index value derived from stable isotopes and concentration.

Spectral features from DRIFTS data and low C:N values are indicative of greater persistence of plant and microbial carbon in subsoils at Angelo. We detected low C:N (<5) values at Angelo compared to Sedgwick and Hopland (Fig. 2c). The C:N ratios of SOC can be influenced by the catabolic and anabolic metabolisms of soil microbes and plant inputs. C:N values throughout the soil profile can reflect the balance of microbial and plant biomass inputs. The production and recycling of metabolites and the

generation of biomass lower the C:N ratios of SOC, but fresh plant inputs can increase the C:N ratios. Thus, the low C:N ratios measured at depth in the soils at Angelo could be caused by greater microbial processing of SOC and necromass at depth in Angelo soils. However, it is important to note that these low C:N ratios are at odds with our DRIFTS results, which suggest the dry and intermediates sites, Sedgwick, and Hopland, respectively, have the greatest proportion of microbially associated organic matter (Fig. 8c). and the greatest microbial oxidation (Fig. 8d). These contrasting results suggest that microbial biomass and necromass could be prevalent at all three sites, and comprise 50% of the total pool across all sites. In fact, necromass has been shown to be a significant portion of SOC in grasslands (Buckeridge et al. 2020, 2022; Liang et al. 2019; B. Wang et al. 2021). Our elemental, isotopic, and spectroscopic measurements were all done on bulk soils, so we are likely observing a combination of inactive microbial biomass, necromass, and plant inputs.

Variance of $\delta^{13}C$ and $\delta^{15}N$ values explained by depth and biotic factors

We observed a strong depth correlation with $\delta^{13}C$ values, but not $\delta^{15}N$ values across the three sampled localities. We hypothesized that $\delta^{13}C$ and $\delta^{15}N$ values would be greatest at our most arid site. However, $\delta^{13}C$ and $\delta^{15}N$ was relatively similar between Angelo and Sedgwick. Sedgwick subsoils had the greatest $\delta^{15}N$ values in subsoils at Sedgwick, which could be influenced by rock derived and inorganic nitrogen (Bingham et al. 2021). While photosynthetic pathways are a key influence on surface $\delta^{13}C$ values, all sites were similarly dominated by C3 vegetation and therefore exhibited similar surface $\delta^{13}C$ values (Table S1). Furthermore, introduced annual grasses with shallow roots dominated our sites (Table S1). Although plant tissue $\delta^{13}C$ is affected by MAP and plants in arid ecosystems often express higher $\delta^{13}C$ (Kohn 2010), the trends between sites are not likely caused by differences in vegetation isotopic composition. While we lack vegetation $\delta^{13}C$ measurements to confirm if we are seeing this effect, surface $\delta^{13}C$ values were very similar across sites (Fig. 2d) vary by < 1‰, and are similar to other C3 dominant grassland sites (Brenner et al. 2001; Schneckenberger and Kuzyakov 2007; Von Fischer et al. 2008; Wedin et al.

1995). In general, $\delta^{13}C$ values increase with depth in soils (Krüger et al. 2023; Natelhoffer and Fry 1988; Staddon 2004); however, Hopland had lower $\delta^{13}C$ values in depths greater than 30 cm, but Angelo and Sedgwick had relatively similar values. At Hopland, the intermediate temperature and precipitation site, we observed the lowest $\delta^{13}C$ values below 30 cm (Fig. 2d) and redoximorphic features at depth (~ 60 to 100 cm). There is emerging evidence that microbial necromass contributes to $\delta^{13}C$ values, especially at depth (Kohl et al. 2015). High $\delta^{13}C$ values are indicative of a greater isotopic fractionation that occurs during microbial carbon recycling and necromass accumulation (Krüger et al. 2023). The redox features at Hopland are evidence of a mixture of oxic and anoxic microsites within soil. These microsites have been shown to have a higher diversity of aerobic and anaerobic microbial metabolisms and metabolites are key in soil carbon stabilization (Keiluweit et al. 2017; Lacroix et al. 2023; Naughton et al. 2023), but the connection between $\delta^{13}C$ values and reactive microsites is not well characterized. This chemical process at Hopland could explain the trend of lower $\delta^{13}C$ values in soil depths greater than 30 cm (Fig. 2d) and the broadest variability in complex plant derived OM at depth (Fig. 8c).

In contrast to our initial hypothesis, we did not observe a strong relationship between $\delta^{15}N$ values across our grassland ecosystems with varying precipitation regimes. This lack of $\delta^{15}N$ variation with climate is consistent with previous findings that suggest that $\delta^{15}N$ is invariant with MAP after controlling for soil carbon and clay content (Craine et al. 2015). These samples were collected during the peak of dry season in Mediterranean grasslands when we would expect lower microbial activity compared to the wet winter season. Studies have found that soil $\delta^{15}N$ values at depth in regions with a distinct wet and dry season are greatly affected by time of sampling (Wang et al. 2009). It is common for grasslands to exhibit a consistent increase of $\delta^{15}N$ values with depth (Amundson et al. 2003) but during the wet season, $\delta^{15}N$ values increase at the surface due to higher levels of microbial activity and ^{14}N loss, which results in ^{15}N enriched substrates (Wang et al. 2009). Another biotic process that can affect $\delta^{15}N$ depth profiles is fungal inputs. Soil $\delta^{15}N$ values at depth integrate many processes and can be dominated by fungal transfer of nitrogen to plants; however,

typical soil processing protocols bias against observing root inputs in samples due to sieving (Hobbie and Ouimette 2009). Bulk soils in ecosystems with arbuscular mycorrhizal (AMF) fungi have $\delta^{15}N$ values of $4.6 \pm 0.5\permil$ and maximum values at intermediate depth (Hobbie and Ouimette 2009). At Hopland, we observed this $\delta^{15}N$ profile pattern consistent with AMF processes. The prevalence of AMF at all three of our study sites is well documented through amplicon sequencing (Hawkes et al. 2011; Treseder et al. 2010; Yuan et al. 2021) but determining the effects of AMF on $\delta^{15}N$ profiles will take further investigation. Lastly, $\delta^{15}N$ values can be affected by abiotic inputs, namely rock derived nitrogen, as documented at Sedgwick where there are high $\delta^{15}N$ values (~6‰) at depths greater than 1 m (Bingham et al. 2021). While our results did not directly indicate rock derived nitrogen at Sedgwick, there were increased $\delta^{15}N$ values at depth and we cannot rule out this impact.

Climatic factors may explain differences in processing index across ecosystems, but not in turnover index

Angelo, Hopland, and Sedgwick represent a climatic gradient of grassland ecosystems and we observed unique patterns in stabilization mechanisms and microbial processing through their depth profiles of C:N and stable isotopes. Stability, or persistence, of soil organic matter has emerged as an important ecosystem property in the current paradigm of soil science research (Schmidt et al. 2011). Relationships between C:N and $\delta^{15}N$ values coincides with measurements of mineral-associated versus particulate organic matter (POM) (Conen et al. 2008). At Angelo, subsoil (>30 cm) SOM was largely differentiated by depth separation of C:N, indicating carbon loss at depth with not much variation in $\delta^{15}N$ (Fig. 6a). More specifically, the differentiation in patterns of C:N and $\delta^{15}N$ values between shallow versus deep soils at Angelo suggests the dominant mechanism of stabilization is through mineral association with iron and aluminum short-range order oxides (Berhe et al. 2012; Foley et al. 2023). In contrast, at Sedgwick, there was a homogenous, continuous $\delta^{15}N$ and C:N association across all depths, with a high variability in $\delta^{15}N$ values and little depth separation (Conen et al. 2008). We interpret this as indicative of greater microbial processing at Sedgwick

and differing stabilization mechanisms at our sites. Sedgwick has a higher pH and higher clay content at the surface (Table 1), and stabilization here is likely driven by organic matter association with polyvalent base cations. Our results also agree with prior studies and strengthen the hypothesis that wetter environments lead to stabilization of organic matter and more MAOM formation (Heckman et al. 2023).

Differences in soil turnover across the study sites, interpreted through the turnover index (β), were decoupled from climatic differences across sites. We observed highest turnover at Sedgwick, our driest site (Fig. 5a). Previous studies indicate an inverse relationship between MAT and β (Brunn et al. 2014); however, Sedgwick and Angelo had similar β values, which is inconsistent with previous studies corresponding increases in β with MAP (Brunn et al. 2014). The majority of previous studies regarding β have been done in temperate forest ecosystems (fig. S3), which likely affects the relationship between β and climate. However, our data fall within expected values for other temperate ecosystems (Fig. S3). Additionally, greater decomposition rate under higher MAP is not consistent in the literature, however our relative turnover times somewhat agree with Foley et al. (2023) that reported radiocarbon (^{14}C) age of surface soils at these same three localities and observed increases in ^{14}C age with MAP. Sedgwick had the greatest turnover index according to β and also the youngest turnover time according to surface radiocarbon. However, we did observe the lowest turnover index at Hopland, while it had an intermediate turnover time according to radiocarbon. These comparisons are also limited due to radiocarbon measurements only being measured in surface soils, whereas β was calculated with the entire depth profile to 1 m. We did an additional analysis of β in just topsoils (0–30 cm) to see if this would have better agreement with radiocarbon measurements, but overall trends were similar when using just topsoils to calculate β (Figure S4; Table S2). These younger soil C ages at Sedgwick provide evidence for greater microbial processing of organic matter at Sedgwick (Foley et al. 2023). $\delta^{13}C$ values are connected to decomposition processes in soils, and can be affected by the interactions between litter quality, microbial respiration, and the physiochemical parameters of soil (Brunn et al. 2014). The increase

in β at Angelo could also be due to leaching of dissolved organic carbon (DOC), which is possible due to its precipitation regime and high relative MAP (Fig. 1a). Increased DOC leaching through the profile can increase β due to the ^{13}C enrichment (Kaiser and Zech 2000); however, recent studies have questioned this ^{13}C enrichment of DOC (Philben et al. 2022). Instead, ^{13}C enrichment is likely dominated by biotic factors, like microbial immobilization, plant uptake, and fungal transport (Philben et al. 2022). High β at Sedgwick is also consistent with our DRIFTS data in Sedgwick subsoils, which suggests greater microbial oxidation in subsoils (Fig. 5) compared to Angelo.

This study combines the geochemical and spectrographic techniques of stable isotope analysis and DRIFTS to determine proxies of processing and turnover of soil carbon, as well as to discern the contributing biological processes. A standard and accepted method for determining stability is splitting SOC into mineral-associated and particulate organic carbon, via a costly and labor-intensive density fractionation methodology (Sollins et al. 2006, 2009). Turnover is commonly assessed through radiocarbon measurements, which is inaccessible to many researchers given the cost and limited availability of specialized instrumentation. Furthermore, the continued decline of bomb curve ^{14}C due to fossil fuel emissions as well as its decay will make interpretations of radiocarbon increasingly complicated into the future (Graven 2015; Sierra 2018). Greater exploration is needed of stable isotope measures of decomposition and persistence. Analysis of elemental concentrations and stable isotope compositions using elemental analyzers coupled to isotope ratio mass spectrometers are increasingly becoming more common and affordable. In contrast to density fractionation and radiocarbon measurement, stable isotope proxies can be used as a high throughput and low-cost way to measure benchmarks for important ecosystem properties like soil turnover and stability. The non-destructive acquisition of DRIFTS data was suitable for detecting regional differences in functional group character between sites and at picking up depth differences (Figs. 7, 8). Combining isotopic proxies and spectroscopic methods can be another powerful and accessible way of understanding carbon and nitrogen dynamics across diverse ecosystems.

Implications for grassland C sequestration

The effect of changing precipitation and temperature patterns on terrestrial carbon cycling will have cascading consequences for soil carbon sequestration (Bai and Cotrufo 2022; Song et al. 2019). Plant communities are affected by both the amount and timing of precipitation. In tall-grass prairie ecosystems, decreases in precipitation result in lower plant diversity (Dennhardt et al. 2021; Fay et al. 2002; Smith et al. 2016). Shifts in diversity as well as increases in invasives annuals in California grasslands are associated with declines in soil carbon storage (Koteen et al. 2011). There is also evidence from Angelo that extending the rainy season into the spring has increased the dominance of invasive annual grasses (Suttle et al. 2007). Overall, this linkage between reduced plant diversity and SOC storage in California grasslands suggests a negative impact on their capacity to sequester atmospheric carbon dioxide. In this study, we illustrated regional differences in SOM processing, turnover, and composition. Although we did not observe large differences in elemental concentration of carbon and nitrogen, we detected differences in the processing of carbon at depth across the sites. These regional differences in baseline processing, turnover, and organic matter composition need to be taken into account for future C sequestration and modeling efforts.

Conclusions

We investigated the SOM processing, turnover, and organic matter composition down to 1 m depths across three Californian grassland ecosystems. Elemental and isotopic analysis reveal that, while there are few differences in carbon and nitrogen abundances in grassland soils, we do see differences in the processing and turnover of SOM across a mean annual precipitation gradient. We applied two natural isotopic abundance proxies as an index for turnover (β) and processing (C:N versus δ^{15}N). We also characterized organic matter composition using Diffuse Reflectance Infrared Fourier Transform Spectroscopy (DRIFTS) to better characterize the plant and microbial character across gradients and depths. Our results found the wettest site had the greatest carbon stock at the surface, likely

mediated by greater plant inputs; however, carbon stock values converged between the wettest and driest site in subsoils. Soil at the driest and hottest site (Sedgwick) has the greatest turnover and most processing. The wettest site (Angelo) had a high degree of processing at depth, likely due to greater mineral association of organic matter at depth. We observed the lowest $\delta^{13}C$ values in subsoils at our intermediate site, despite expecting the greatest values at our driest site. Our results highlight regional variability in SOM processing and turnover across climatic gradients. The contrasting results between topsoils and subsoils demonstrate the importance of understanding both regional differences and patterns with depth across a climatic gradient of California grasslands.

Author contributions Material preparation, sample collection, data collection, and analysis were performed by Leila Wahab. The first draft of the manuscript was written by Leila Wahab, and all authors comments on previous versions of the manuscript. All authors read and approved the final manuscript.

Data availability All of the data used for this study, including meta data and soil elemental/isotopic data, is available in the Dryad Open data repository (preliminary link that is private until the manuscript is published: https://datadryad.org/stash/share/qWsU4uKfHSePzs54nP24rrUhRNbLCz0htfUPoRK9qd0).

Declarations

Conflict of interest All authors declare they have no competing financial interests.

References

Abdelbaki AM (2018) Evaluation of pedotransfer functions for predicting soil bulk density for U.S. soils. Ain Shams Eng J 9(4):1611–1619. https://doi.org/10.1016/j.asej.2016.12.002

Acton P, Fox C, Rowe H, Wilkinson M (2013) Carbon isotopes for estimating soil decomposition and physical mixing in well-drained forest soils. JGR Biogeosciences 118:1532–1545. https://doi.org/10.1002/2013JG002400

Agnihotri R, Mandal TK, Karapurkar SG, Naja M, Gadi R, Ahammmed YN, Kumar A, Saud T, Saxena M (2011) Stable carbon and nitrogen isotopic composition of bulk aerosols over India and northern Indian Ocean. Atmos Environ 45(17):2828–2835. https://doi.org/10.1016/j.atmosenv.2011.03.003

Alexander EB (1980) Bulk densities of California soils in relation to other soil properties. Soil Sci Soc Am J 44(4):689–692. https://doi.org/10.2136/sssaj1980.03615995004400040005x

Amundson R, Austin AT, Schuur EAG, Yoo K, Matzek V, Kendall C, Uebersax A, Brenner D, Baisden WT (2003) Global patterns of the isotopic composition of soil and plant nitrogen. Global Biogeochem Cycles. https://doi.org/10.1029/2002GB001903

Aquino AJA, Tunega D, Schaumann GE, Haberhauer G, Gerzabek MH, Lischka H (2011) The functionality of cation bridges for binding polar groups in soil aggregates. Int J Quantum Chem 111(7–8):1531–1542. https://doi.org/10.1002/qua.22693

Aranibar JN, Otter L, Macko SA, Feral CJW, Epstein HE, Dowty PR, Eckardt F, Shugart HH, Swap RJ (2004) Nitrogen cycling in the soil-plant system along a precipitation gradient in the Kalahari sands: nitrogen cycling in the Kalahari. Glob Change Biol 10(3):359–373. https://doi.org/10.1111/j.1365-2486.2003.00698.x

Bai Y, Cotrufo MF (2022) Grassland soil carbon sequestration: current understanding, challenges, and solutions. Science 377(6606):603–608. https://doi.org/10.1126/science.abo2380

Berhe A, Suttle KB, Burton SD, Banfield JF (2012) Contingency in the direction and mechanics of soil organic matter responses to increased rainfall. Plant Soil 358:371–383

Berthrong ST, Piñeiro G, Jobbágy EG, Jackson RB (2012) Soil C and N changes with afforestation of grasslands across gradients of precipitation and plantation age. Ecol Appl 22(1):76–86. https://doi.org/10.1890/10-2210.1

Bingham NL, Slessarev EW, Homyak PM, Chadwick OA (2021) Rock-sourced nitrogen in semi-arid, shale-derived California soils. Front for Global Change 4:672522. https://doi.org/10.3389/ffgc.2021.672522

Brenner DL, Amundson R, Baisden WT, Kendall C, Harden J (2001) Soil N and 15 N variation with time in a California annual grassland ecosystem. Geochim Cosmochim Acta 65(22):4171–4186. https://doi.org/10.1016/S0016-7037(01)00699-8

Brunn M, Spielvogel S, Sauer T, Oelmann Y (2014) Temperature and precipitation effects on δ13C depth profiles in SOM under temperate beech forests. Geoderma 235–236:146–153. https://doi.org/10.1016/j.geoderma.2014.07.007

Brunn M, Condron L, Wells A, Spielvogel S, Oelmann Y (2016) Vertical distribution of carbon and nitrogen stable isotope ratios in topsoils across a temperate rainforest dune chronosequence in New Zealand. Biogeochemistry 129(1–2):37–51. https://doi.org/10.1007/s10533-016-0218-4

Buckeridge KM, La Rosa AF, Mason KE, Whitaker J, McNamara NP, Grant HK, Ostle NJ (2020) Sticky dead microbes: rapid abiotic retention of microbial necromass in soil. Soil Biol Biochem 149:107929. https://doi.org/10.1016/j.soilbio.2020.107929

Buckeridge KM, Mason KE, Ostle N, McNamara NP, Grant HK, Whitaker J (2022) Microbial necromass carbon and nitrogen persistence are decoupled in agricultural grassland soils. Commun Earth Environ 3(1):114. https://doi.org/10.1038/s43247-022-00439-0

Button ES, Pett-Ridge J, Murphy DV, Kuzyakov Y, Chadwick DR, Jones DL (2022) Deep-C storage: biological, chemical and physical strategies to enhance carbon stocks in agricultural subsoils. Soil Biol Biochem 170:108697. https://doi.org/10.1016/j.soilbio.2022.108697

Campbell JE, Fox JF, Davis CM, Rowe HD, Thompson N (2009) Carbon and nitrogen isotopic measurements from southern Appalachian soils: assessing soil carbon sequestration under climate and land-use variation. J Environ Eng 135(6):439–448. https://doi.org/10.1061/(ASCE)EE.1943-7870.0000008

Campo J, Merino A (2016) Variations in soil carbon sequestration and their determinants along a precipitation gradient in seasonally dry tropical forest ecosystems. Glob Change Biol 22(5):1942–1956. https://doi.org/10.1111/gcb.13244

Chai H, Li J, Ochoa-Hueso R, Yang X, Li J, Meng B, Song W, Zhong X, Ma J, Sun W (2022) Different drivers of soil C accumulation in aggregates in response to altered precipitation in a semiarid grassland. Sci Total Environ 830:154760. https://doi.org/10.1016/j.scitotenv.2022.154760

Chen J, Elsgaard L, Van Groenigen KJ, Olesen JE, Liang Z, Jiang Y, Lærke PE, Zhang Y, Luo Y, Hungate BA, Sinsabaugh RL, Jørgensen U (2020a) Soil carbon loss with warming: new evidence from carbon-degrading enzymes. Glob Change Biol 26(4):1944–1952. https://doi.org/10.1111/gcb.14986

Chen J, van Groenigen KJ, Hungate BA, Terrer C, van Groenigen J-W, Maestre FT, Ying SC, Luo Y, Jørgensen U, Sinsabaugh RL (2020b) Long-term nitrogen loading alleviates phosphorus limitation in terrestrial ecosystems. Glob Change Biol 26(9):5077–5086

Chou WW, Silver WL, Jackson RD, Thompson AW, Allen-Diaz B (2008) The sensitivity of annual grassland carbon cycling to the quantity and timing of rainfall. Glob Change Biol 14(6):1382–1394. https://doi.org/10.1111/j.1365-2486.2008.01572.x

Conen F, Zimmermann M, Leifeld J, Seth B, Alewell C (2008) Relative stability of soil carbon revealed by shifts in δ15N and C: N ratio. Biogeosciences 5(1):123–128

Conen F, Yakutin MV, Carle N, Alewell C (2013) δ 15 N natural abundance may directly disclose perturbed soil when related to C: N ratio: δ15 N natural abundance to directly disclose perturbed soil. Rapid Commun Mass Spectrom 27(10):1101–1104. https://doi.org/10.1002/rcm.6552

Craine JM, Elmore AJ, Wang L, Augusto L, Baisden WT, Brookshire ENJ, Cramer MD, Hasselquist NJ, Hobbie EA, Kahmen A, Koba K, Kranabetter JM, Mack MC, Marin-Spiotta E, Mayor JR, McLauchlan KK, Michelsen A, Nardoto GB, Oliveira RS et al (2015) Convergence of soil nitrogen isotopes across global climate gradients. Sci Rep 5(1):8280. https://doi.org/10.1038/srep08280

D'Antonio C, Bainbridge S, Kennedy C, Bartolome J, Reynolds S (2002) Ecology and restoration of California grasslands with special emphasis on the influence of fire and grazing on native grassland species. In: Report to the Packard foundation, 99.

Deepika S, Kothamasi D (2015) Soil moisture—a regulator of arbuscular mycorrhizal fungal community assembly and symbiotic phosphorus uptake. Mycorrhiza 25(1):67–75. https://doi.org/10.1007/s00572-014-0596-1

Dennhardt LA, Aldrich-Wolfe L, Black KL, Shivega WG, Travers SE (2021) Forty years of increasing precipitation is correlated with loss of forbs in a tallgrass prairie. Nat Areas J. https://doi.org/10.3375/043.041.0305

Dijkstra P, LaViolette CM, Coyle JS, Doucett RR, Schwartz E, Hart SC, Hungate BA (2008) 15N enrichment as an integrator of the effects of C and N on microbial metabolism and ecosystem function. Ecol Lett 11(4):389–397. https://doi.org/10.1111/j.1461-0248.2008.01154.x

Ehleringer JR, Buchmann N, Flanagan LB (2000) Carbon isotope ratios in belowground carbon cycle processes. Ecol Appl 10(2):412–422. https://doi.org/10.1890/1051-0761(2000)010[0412:CIRIBC]2.0.CO;2

Farquhar GD, Ehleringer JR, Hubick KT (1989) Carbon isotope discrimination and photosynthesis. Annu Rev Plant Physiol Plant Mol Biol 40:503–537

Fay PA, Carlisle JD, Danner BT, Lett MS, McCarron JK, Stewart C, Knapp AK, Blair JM, Collins SL (2002) Altered rainfall patterns, gas exchange, and growth in grasses and

forbs. Int J Plant Sci 163(4):549–557. https://doi.org/10.1086/339718

Foley MM, Blazewicz SJ, McFarlane KJ, Greenlon A, Hayer M, Kimbrel JA, Koch BJ, Monsaint-Queeney VL, Morrison K, Morrissey E, Hungate BA, Pett-Ridge J (2023) Active populations and growth of soil microorganisms are framed by mean annual precipitation in three California annual grasslands. Soil Biol Biochem 177:108886. https://doi.org/10.1016/j.soilbio.2022.108886

Fröberg M, Hanson PJ, Todd DE, Johnson DW (2008) Evaluation of effects of sustained decadal precipitation manipulations on soil carbon stocks. Biogeochemistry 89(2):151–161. https://doi.org/10.1007/s10533-008-9205-8

Garten CT (2006) Relationships among forest soil C isotopic composition, partitioning, and turnover times. Can J for Res 36:2157–2167

Garten CT, Hanson PJ (2006) Measured forest soil C stocks and estimated turnover times along an elevation gradient. Geoderma 136(1–2):342–352. https://doi.org/10.1016/j.geoderma.2006.03.049

Grant KE, Hilton RG, Galy VV (2023) Global patterns of radiocarbon depletion in subsoil linked to rock-derived organic carbon. Geochem Perspect Lett 25:36–40. https://doi.org/10.7185/geochemlet.2312

Graven HD (2015) Impact of fossil fuel emissions on atmospheric radiocarbon and various applications of radiocarbon over this century. Proc Natl Acad Sci 112(31):9542–9545. https://doi.org/10.1073/pnas.1504467112

Harper CW, Blair JM, Fay PA, Knapp AK, Carlisle JD (2005) Increased rainfall variability and reduced rainfall amount decreases soil CO_2 flux in a grassland ecosystem. Glob Change Biol 11(2):322–334. https://doi.org/10.1111/j.1365-2486.2005.00899.x

Hartman G, Danin A (2010) Isotopic values of plants in relation to water availability in the Eastern Mediterranean region. Oecologia 162(4):837–852. https://doi.org/10.1007/s00442-009-1514-7

Hawkes CV, Kivlin SN, Rocca JD, Huguet V, Thomsen MA, Suttle KB (2011) Fungal community responses to precipitation. Glob Change Biol 17(4):1637–1645. https://doi.org/10.1111/j.1365-2486.2010.02327.x

Heckman KA, Possinger AR, Badgley BD, Bowman MM, Gallo AC, Hatten JA, Nave LE, SanClements MD, Swanston CW, Weiglein TL, Wieder WR, Strahm BD (2023) Moisture-driven divergence in mineral-associated soil carbon persistence. Proc Natl Acad Sci 120(7):e2210044120. https://doi.org/10.1073/pnas.2210044120

Hicks Pries CE, Ryals R, Zhu B, Min K, Cooper A, Goldsmith S, Pett-Ridge J, Torn M, Berhe AA (2023) The deep soil organic carbon response to global change. Annu Rev Ecol Evol Syst 54(1):375–401. https://doi.org/10.1146/annurev-ecolsys-102320-085332

Hobbie EA, Ouimette AP (2009) Controls of nitrogen isotope patterns in soil profiles. Biogeochemistry 95(2–3):355–371. https://doi.org/10.1007/s10533-009-9328-6

Högberg P (1997) 15N natural abundance in soil–plant systems. New Phytol 137(2):179–203

IPCC (2022) Water. In: Climate change 2022: impacts, adaptation, and vulnerability. Contribution of Working Group II to the sixth assessment report of the intergovernmental panel on climate change.

Jia J, Cao Z, Liu C, Zhang Z, Lin L, Wang Y, Haghipour N, Wacker L, Bao H, Dittmar T, Simpson MJ, Yang H, Crowther TW, Eglinton TI, He J, Feng X (2019) Climate warming alters subsoil but not topsoil carbon dynamics in alpine grassland. Glob Change Biol 25(12):4383–4393. https://doi.org/10.1111/gcb.14823

Jilling A, Keiluweit M, Contosta AR, Frey S, Schimel J, Schnecker J, Smith RG, Tiemann L, Grandy AS (2018) Minerals in the rhizosphere: overlooked mediators of soil nitrogen availability to plants and microbes. Biogeochemistry 139(2):103–122. https://doi.org/10.1007/s10533-018-0459-5

Jobbágy EG, Jackson RB (2000) The vertical distribution of soil organic carbon and its relation to climate and vegetation. Ecol Appl 10(2):423–436. https://doi.org/10.1890/1051-0761(2000)010[0423:TVDOSO]2.0.CO;2

Kaiser K, Zech W (2000) Sorption of dissolved organic nitrogen by acid subsoil horizons and individual mineral phases. Eur J Soil Sci 51(3):403–411. https://doi.org/10.1046/j.1365-2389.2000.00320.x

Keiluweit M, Bougoure JJ, Nico PS, Pett-Ridge J, Weber PK, Kleber M (2015) Mineral protection of soil carbon counteracted by root exudates. Nat Clim Chang 5(6):588–595. https://doi.org/10.1038/nclimate2580

Keiluweit M, Wanzek T, Kleber M, Nico P, Fendorf S (2017) Anaerobic microsites have an unaccounted role in soil carbon stabilization. Nat Commun 8(1):1771. https://doi.org/10.1038/s41467-017-01406-6

Knapp AK (2002) Rainfall variability, carbon cycling, and plant species diversity in a mesic grassland. Science 298(5601):2202–2205. https://doi.org/10.1126/science.1076347

Kögel-Knabner I, Amelung W (2014) Dynamics, chemistry, and preservation of organic matter in soils. Treatise on geochemistry. Elsevier, New York, pp 157–215

Kohl L, Laganière J, Edwards KA, Billings SA, Morrill PL, Van Biesen G, Ziegler SE (2015) Distinct fungal and bacterial $\delta^{13}C$ signatures as potential drivers of increasing δ13C of soil organic matter with depth. Biogeochemistry 124(1–3):13–26. https://doi.org/10.1007/s10533-015-0107-2

Kohn MJ (2010) Carbon isotope compositions of terrestrial C3 plants as indicators of (paleo)ecology and (paleo)climate. Proc Natl Acad Sci 107(46):19691–19695. https://doi.org/10.1073/pnas.1004933107

Koteen LE, Baldocchi DD, Harte J (2011) Invasion of nonnative grasses causes a drop in soil carbon storage in California grasslands. Environ Res Lett 6(4):044001. https://doi.org/10.1088/1748-9326/6/4/044001

Krüger N, Finn DR, Don A (2023) Soil depth gradients of organic carbon-13—a review on drivers and processes. Plant Soil. https://doi.org/10.1007/s11104-023-06328-5

Lacroix EM, Aeppli M, Boye K, Brodie E, Fendorf S, Keiluweit M, Naughton HR, Noël V, Sihi D (2023) Consider the anoxic microsite: acknowledging and appreciating spatiotemporal redox heterogeneity in soils and sediments. ACS Earth Space Chemistry 7(9):1592–1609. https://doi.org/10.1021/acsearthspacechem.3c00032

Liang C, Amelung W, Lehmann J, Kästner M (2019) Quantitative assessment of microbial necromass contribution

to soil organic matter. Glob Change Biol 25(11):3578–3590. https://doi.org/10.1111/gcb.14781

M M a i n k a L S u m m e r a u e r D W a s n e r G G a r-landMGriepentrogAABerheSDoetterl2021Soil geochemistry as a driver of soil organic matter composition: insights from a soil chronosequenceBiogeochemistry10.5194/bg-2021-295Mainka M, Summerauer L, Wasner D, Garland G, Griepentrog M, Berhe AA, Doetterl S (2021) Soil geochemistry as a driver of soil organic matter composition: insights from a soil chronosequence. Biogeochemistry. https://doi.org/10.5194/bg-2021-295

Margenot A, Calderón F, Parikh SJ (2015) Limitations and potential of spectral subtractions in fourier-transform infrared spectroscopy of soil samples. Soil Sci Soc Am J 80:10–26. https://doi.org/10.2136/sssaj2015.06.0228

Natelhoffer KJ, Fry B (1988) Controls on natural nitrogen-15 and carbon-13 abundances in forest soil organic matter. Soil Sci Soc Am J 52(6):1633–1640

Naughton HR, Tolar BB, Dewey C, Keiluweit M, Nico PS, Fendorf S (2023) Reactive iron, not fungal community, drives organic carbon oxidation potential in floodplain soils. Soil Biol Biochem 178:108962. https://doi.org/10.1016/j.soilbio.2023.108962

Parikh SJ, Goyne KW, Margenot AJ, Mukome FND, Calderón FJ (2014) Soil chemical insights provided through vibrational spectroscopy. Advances in agronomy, vol 126. Elsevier, New York, pp 1–148

Philben M, Bowering K, Podrebarac FA, Laganière J, Edwards K, Ziegler SE (2022) Enrichment of 13C with depth in soil organic horizons is not explained by CO_2 or DOC losses during decomposition. Geoderma 424:116004. https://doi.org/10.1016/j.geoderma.2022.116004

Robinson D (2001) $\delta^{15}N$ as an integrator of the nitrogen cycle. Trends Ecol Evol 16(3):153–162. https://doi.org/10.1016/S0169-5347(00)02098-X

Rocci KS, Lavallee JM, Stewart CE, Cotrufo MF (2021) Soil organic carbon response to global environmental change depends on its distribution between mineral-associated and particulate organic matter: a meta-analysis. Sci Total Environ 793:148569. https://doi.org/10.1016/j.scitotenv.2021.148569

Rumpel C (2004) Location and chemical composition of stabilized organic carbon in topsoil and subsoil horizons of two acid forest soils. Soil Biol Biochem 36(1):177–190. https://doi.org/10.1016/j.soilbio.2003.09.005

Ryals R, Kaiser M, Torn MS, Berhe AA, Silver WL (2014) Impacts of organic matter amendments on carbon and nitrogen dynamics in grassland soils. Soil Biol Biochem 68:52–61. https://doi.org/10.1016/j.soilbio.2013.09.011

Schmidt MWI, Torn MS, Abiven S, Dittmar T, Guggenberger G, Janssens IA, Kleber M, Kögel-Knabner I, Lehmann J, Manning DAC, Nannipieri P, Rasse DP, Weiner S, Trumbore SE (2011) Persistence of soil organic matter as an ecosystem property. Nature 478(7367):49–56. https://doi.org/10.1038/nature10386

Schneckenberger K, Kuzyakov Y (2007) Carbon sequestration under *Miscanthus* in sandy and loamy soils estimated by natural ^{13}C abundance. J Plant Nutr Soil Sci 170(4):538–542. https://doi.org/10.1002/jpln.200625111

Sierra CA (2018) Forecasting atmospheric radiocarbon decline to pre-bomb values. Radiocarbon 60(4):1055–1066. https://doi.org/10.1017/RDC.2018.33

Smith NG, Schuster MJ, Dukes JS (2016) Rainfall variability and nitrogen addition synergistically reduce plant diversity in a restored tallgrass prairie. J Appl Ecol 53(2):579–586. https://doi.org/10.1111/1365-2664.12593

Sokol NW, Whalen E, Jilling A, Kallenbach CM, Pett-Ridge J, Georgiou K (2022) Global distribution, formation and fate of mineral-associated soil organic matter under a changing climate: a trait-based perspective. Funct Ecol 36:1411–1429. https://doi.org/10.1111/1365-2435.14040

Sollins P, Swanston C, Kleber M, Filley T, Kramer M, Crow S, Caldwell BA, Lajtha K, Bowden R (2006) Organic C and N stabilization in a forest soil: evidence from sequential density fractionation. Soil Biol Biochem 38(11):3313–3324. https://doi.org/10.1016/j.soilbio.2006.04.014

Sollins P, Kramer MG, Swanston C, Lajtha K, Filley T, Aufdenkampe AK, Wagai R, Bowden RD (2009) Sequential density fractionation across soils of contrasting mineralogy: evidence for both microbial- and mineral-controlled soil organic matter stabilization. Biogeochemistry 96(1–3):209–231. https://doi.org/10.1007/s10533-009-9359-z

Song J, Wan S, Piao S, Knapp AK, Classen AT, Vicca S, Ciais P, Hovenden MJ, Leuzinger S, Beier C, Kardol P, Xia J, Liu Q, Ru J, Zhou Z, Luo Y, Guo D, Adam Langley J, Zscheischler J et al (2019) A meta-analysis of 1,119 manipulative experiments on terrestrial carbon-cycling responses to global change. Nat Ecol Evol 3(9):1309–1320. https://doi.org/10.1038/s41559-019-0958-3

Staddon PL (2004) Carbon isotopes in functional soil ecology. Trends Ecol Evol 19(3):148–154. https://doi.org/10.1016/j.tree.2003.12.003

Suttle KB, Thomsen MA (2007) Climate change and grassland restoiration in California: lessons from six years of rainfall manipulation in a North Coast Grassland. Madroño 54(3):225–233. https://doi.org/10.3120/0024-9637(2007)54[225:CCAGRI]2.0.CO;2

Suttle KB, Thomsen MA, Power ME (2007) Species interactions reverse grassland responses to changing climate. Science 315(5812):640–642. https://doi.org/10.1126/science.1136401

Terrer C, Phillips RP, Hungate BA, Rosende J, Pett-Ridge J, Craig ME, van Groenigen KJ, Keenan TF, Sulman BN, Stocker BD, Reich PB, Pellegrini AFA, Pendall E, Zhang H, Evans RD, Carrillo Y, Fisher JB, Van Sundert K, Vicca S, Jackson RB (2021) A trade-off between plant and soil carbon storage under elevated CO_2. Nature 591(7851):599–603. https://doi.org/10.1038/s41586-021-03306-8

Throop HL, Archer SR, Monger HC, Waltman S (2012) When bulk density methods matter: implications for estimating soil organic carbon pools in rocky soils. J Arid Environ 77:66–71. https://doi.org/10.1016/j.jaridenv.2011.08.020

Treseder KK, Schimel JP, Garcia MO, Whiteside MD (2010) Slow turnover and production of fungal hyphae during a Californian dry season. Soil Biol Biochem 42(9):1657–1660. https://doi.org/10.1016/j.soilbio.2010.06.005

Von Fischer JC, Tieszen LL, Schimel DS (2008) Climate controls on C 3 vs. C 4 productivity in North American grasslands from carbon isotope composition of soil organic

matter. Global Change Biol 14(5):1141–1155. https://doi.org/10.1111/j.1365-2486.2008.01552.x

Vranova V, Rejsek K, Formanek P (2013) Aliphatic, cyclic, and aromatic organic acids, vitamins, and carbohydrates in soil: a review. Sci World J 2013:1–15. https://doi.org/10.1155/2013/524239

Wang L, D'Odorico P, Okin GS, Macko SA (2009) Isotope composition and anion chemistry of soil profiles along the Kalahari Transect. J Arid Environ 73(4–5):480–486. https://doi.org/10.1016/j.jaridenv.2008.11.010

Wang C, Houlton BZ, Liu D, Hou J, Cheng W, Bai E (2018) Stable isotopic constraints on global soil organic carbon turnover. Biogeosciences 15(4):987–995. https://doi.org/10.5194/bg-15-987-2018

Wang B, An S, Liang C, Liu Y, Kuzyakov Y (2021) Microbial necromass as the source of soil organic carbon in global ecosystems. Soil Biol Biochem 162:108422. https://doi.org/10.1016/j.soilbio.2021.108422

Wedin DA, Tieszen LL, Dewey B, Pastor J (1995) Carbon isotope dynamics during grass decomposition and soil organic matter formation. Ecology 76(5):1383–1392. https://doi.org/10.2307/1938142

Yost JL, Hartemink AE (2020) How deep is the soil studied—an analysis of four soil science journals. Plant Soil 452(1–2):5–18. https://doi.org/10.1007/s11104-020-04550-z

Yuan MM, Kakouridis A, Starr E, Nguyen N, Shi S, Pett-Ridge J, Nuccio E, Zhou J, Firestone M (2021) Fungal-bacterial cooccurrence patterns differ between arbuscular mycorrhizal fungi and nonmycorrhizal fungi across soil niches. mBio 12(2):e03509-20. https://doi.org/10.1128/mBio.03509-20

Zhang K, Dang H, Zhang Q, Cheng X (2015) Soil carbon dynamics following land-use change varied with temperature and precipitation gradients: evidence from stable isotopes. Glob Change Biol 21(7):2762–2772. https://doi.org/10.1111/gcb.12886